MHD transient flows and heat transfer of dusty fluid in a channel with variable physical properties and Navier slip condition

O.D. Makinde [a,*], T. Chinyoka [b]

[a] Faculty of Engineering, Cape Peninsula University of Technology, P.O. Box 1906, Bellville 7535, South Africa
[b] Center for Research in Computational and Applied Mechanics, University of Cape Town, Rondebosch 7701, South Africa

ARTICLE INFO

ABSTRACT

In this paper, we study the unsteady flow and heat transfer of a dusty fluid between two parallel plates with variable viscosity and electric conductivity. The fluid is driven by a constant pressure gradient and an external uniform magnetic field is applied perpendicular to the plates with a Navier slip boundary condition. The governing non-linear partial differential equations are solved numerically using a semi-implicit finite difference scheme. The effect of the wall slip parameter, viscosity and electric conductivity variation and the uniform magnetic field on the velocity and temperature fields for both the fluid and dust particles is discussed.

1. Introduction

Studies related to flow and heat transfer of dusty fluids in a channel with wall slip are extremely useful in improving the design and operation of many industrial and engineering devices. It has important applications in the fields of fluidization, combustion, use of dust in gas cooling systems, centrifugal separation of matter from fluid, petroleum industry, purification of crude oil, electrostatic precipitation, polymer technology, and fluid droplet sprays [1–6]. The flow of a dusty and electrically conducting fluid through a channel in the presence of a transverse magnetic field is also encountered in a variety of applications such as magnetohydrodynamic (MHD) generators, pumps, accelerators, and flow meters. In these devices, the solid particles in the form of ash or soot are suspended in the conducting fluid as a result of the corrosion and wear activities and/or the combustion processes in MHD generators and plasma MHD accelerators. The resultant effects of the presence of solid particles on the performance of such devices has led to studies of particulate suspensions in conducting fluids in the presence of an externally applied magnetic field [7–9].

For the MHD flow of incompressible Newtonian fluids, the governing field equations are the incompressible continuity equation, the Navier–Stokes equations and the energy equation. In addition, a boundary condition has to be imposed on the field equations. Traditionally the so-called no-slip boundary condition is used, namely the fluid velocity relative to the solid is zero on the fluid–solid interface [10]. However, the no-slip condition is a hypothesis rather than a condition deduced from any principle, and thus its validity has been continuously debated in the scientific literature. Although many experimental results were shown to support the no-slip condition including those by Coulomb and Couette, evidences of slip of a fluid on a solid surface were also reported by many others [11]. To describe the slip characteristics of fluid on the solid surface, Navier introduced a more general boundary condition, namely the fluid velocity component tangential to the solid surface, relative to the solid surface, is proportional to the shear stress on the fluid–solid interface. The proportionality is called the slip length which describes the "slipperiness" of the surface [12]. Although Navier's slip condition was proposed about two hundred

* Corresponding author. Tel.: +27 219596641; fax: +27 21 5550775.
   E-mail addresses: makinded@cput.ac.za (O.D. Makinde), tchinyok@vt.edu (T. Chinyoka).
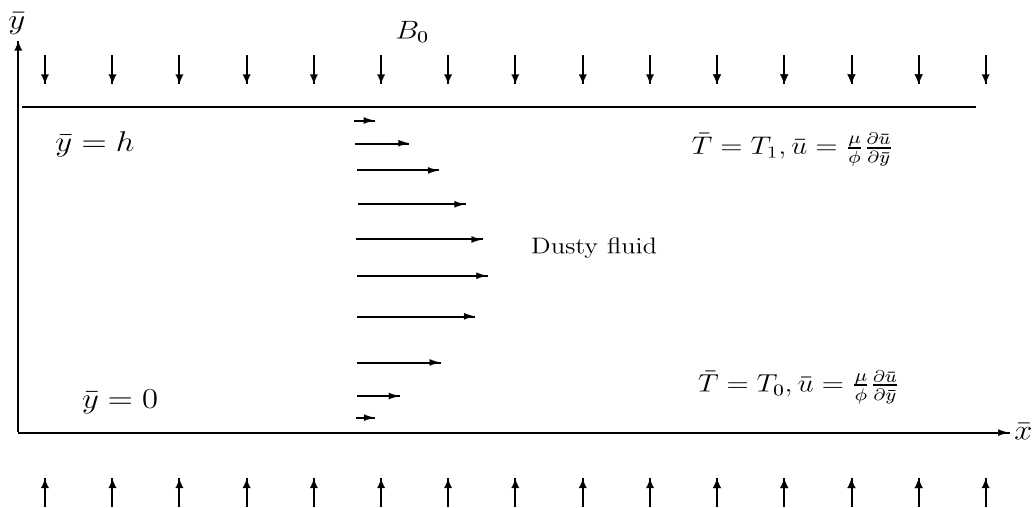
Fig. 1. Schematic diagram of the problem.

years ago, it attracted significant attention of the scientific and engineering communities only very recently for the study of flows on the micro-scale. Recent advances in the manufacture of micro-devices enable experimental investigation of fluid flow on the micro-scale, and many experimental results have provided evidence to support the Navier slip condition [13]. Some attempts have also been made to use nano-technologies for the surface treatment of micro-channels so as to achieve large slip for maximizing the transport efficiency of fluids through them. Over the last few years, various investigations have also been made to study various flow problems of Newtonian and non-Newtonian fluids with or without the Navier slip boundary condition [14–16]. Moreover, accurate prediction for the flow and heat transfer can be achieved by taking into account the variation of these properties with temperature [17]. Attia [8] studied the unsteady MHD flow and heat transfer between two parallel plates with temperature dependent viscosity and thermal conductivity.

In the present work, the unsteady flow and heat transfer of an electrically conducting, incompressible dusty fluid with temperature dependent viscosity and thermal conductivity are studied. The fluid flows between two electrically insulated infinite plates maintained at two constant but different temperatures with the Navier wall slip condition. The fluid is acted upon by a constant pressure gradient and an external uniform magnetic field is applied perpendicular to the plates. The magnetic Reynolds number is assumed very small so that the induced magnetic field is neglected. This configuration is a good approximation of some practical situations such as heat exchangers, flow meters, and pipes that connect system components. The dusty-fluid equations discussed by [1–8] are employed, both the fluid and dust particles are governed by the coupled set of the momentum and energy equations. The Joule effect and viscous dissipation are taken into consideration in the energy equation. The governing coupled nonlinear partial differential equations are solved numerically using semi-implicit finite difference methods. The effects of the external uniform magnetic field, wall slip parameter and the variable viscosity and thermal conductivity on the time development of the velocity and temperature distributions for both the fluid and dust particles are discussed.

2. Mathematical model

We consider an unsteady flow of a dusty conducting fluid between two infinite horizontal plates located at the $y = 0, h$ planes. The dust particles are assumed to be spherical in shape and uniformly distributed throughout the fluid. The two plates are assumed to be kept at two constant temperatures T_0 for the lower plate and T_1 for the upper plate with $T_1 > T_0$, (see Fig. 1).

A constant pressure gradient is applied in the x-direction and a uniform magnetic field B_0 is applied in the positive y-direction. By assuming a very small magnetic Reynolds number the induced magnetic field is neglected [9]. The fluid motion starts from rest at $t = 0$, and the Navier slip condition at the plates implies that the fluid axial velocity component at the plate surface is proportional to the shear stress on the fluid–plate interface. The initial temperature of both the fluid and dust particles is assumed to be equal to T_0. Both the fluid viscosity and the electric conductivity are assumed to vary with temperature. The particle phase is assumed to be stress free, such as in dilute suspensions, and the hydrodynamic interactions between the phases are limited to the drag force. Other interactions such as the virtual mass force, the shear force, and the spin-lift force are assumed to be negligible compared to the drag force [2–4]. This assumption is feasible when the particle Reynolds number is assumed to be small. Following [1–8], the simplified dimensionless governing equations of momentum and energy balance, together with their corresponding boundary conditions, are given as:

$$\frac{\partial u}{\partial t} = \alpha + \frac{1}{\text{Re}} \frac{\partial}{\partial y}\left(\mu(T) \frac{\partial u}{\partial y}\right) - \frac{\text{Ha}^2}{\text{Re}} u - \frac{R}{\text{Re}}(u - u_p), \tag{1}$$
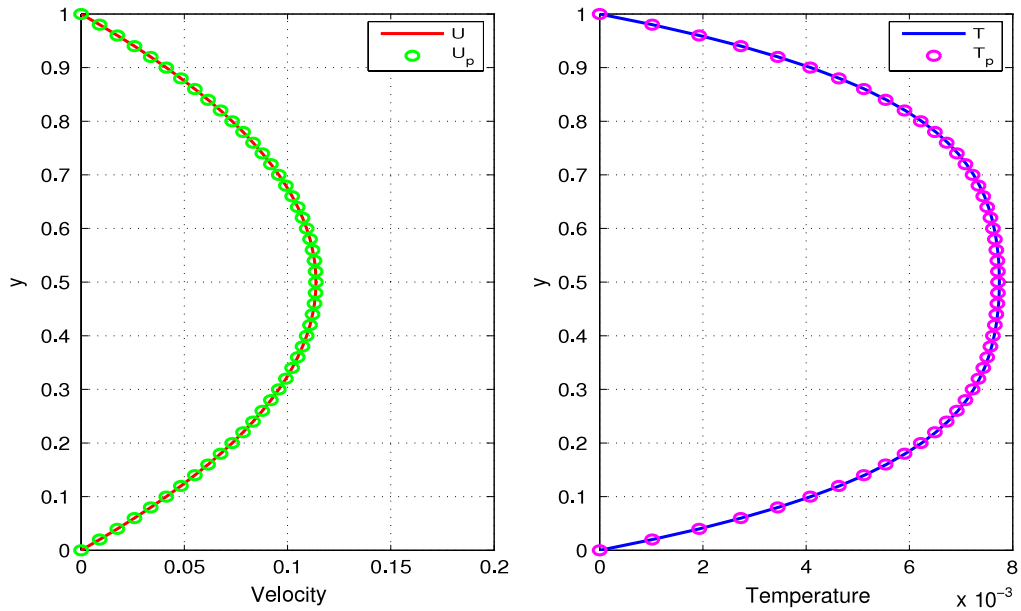
Fig. 2. Solutions with no-slip velocity and zero wall temperature.

$$\frac{\partial u_p}{\partial t} = \frac{1}{\text{Re}\,G}(u - u_p),\tag{2}$$

$$\frac{\partial T}{\partial t} = \frac{1}{\text{Re}\,\text{Pr}}\frac{\partial}{\partial y}\left(\kappa(T)\frac{\partial T}{\partial y}\right) + \frac{\text{Ec}}{\text{Re}}\mu(T)\left(\frac{\partial u}{\partial y}\right)^2 + \frac{\text{Ec}}{\text{Re}}\text{Ha}^2 u^2 + \frac{2R}{3\,\text{Re}\,\text{Pr}}\text{Re}(T_p - T),\tag{3}$$

$$\frac{\partial T_p}{\partial t} = -L(T_p - T),\tag{4}$$

with

$$u(y, t) = u_p(y, t) = T(y, t) = T_p(y, t) = 0, \quad \text{for } t \le 0,\tag{5}$$

$$u_p(0, t) = u_p(1, t) = T_p(0, t) = T(0, t) = 0, \quad \text{for } t > 0,\tag{6}$$

$$\beta\frac{\partial u}{\partial y} = u, \quad \text{for } y = 0, 1, t > 0,\tag{7}$$

$$T_p(1, t) = T(1, t) = 1, \quad \text{for } t > 0,\tag{8}$$

where the temperature dependence of the viscosity and thermal conductivity is modelled as:

$$\mu(T) = \exp(-aT), \qquad \kappa(T) = \exp(bT).\tag{9}$$

In simplifying Eqs. (1)–(9), we have used the following dimensionless quantities:

$$
\begin{aligned}
&x = \frac{\bar{x}}{h}, \qquad y = \frac{\bar{y}}{h}, \qquad t = \frac{U\bar{t}}{h}, \qquad u = \frac{\bar{u}}{U}, \qquad u_p = \frac{\bar{u}_p}{U},\\
&\alpha = -\frac{dP}{dx}, \qquad T = \frac{\bar{T} - T_0}{T_1 - T_0}, \qquad T_p = \frac{\bar{T}_p - T_0}{T_1 - T_0}, \qquad \text{Ha}^2 = \frac{\sigma B_0^2 h^2}{\mu_0},\\
&R = \frac{KNh^2}{\mu_0}, \qquad L = \frac{\rho h^2}{\mu_0\gamma_T}, \qquad \text{Ec} = \frac{U^2}{c_p(T_1 - T_0)}, \qquad a = a_0(T_1 - T_0),\\
&b = b_0(T_1 - T_0), \qquad \text{Pr} = \frac{\mu_0 c_p}{\kappa_0}, \qquad G = \frac{\mu_0}{Nh^2}, \qquad \text{Re} = \frac{\rho U h}{\mu_0}, \qquad \beta = \frac{\mu}{\phi},
\end{aligned}\tag{10}
$$

where T is the temperature of the fluid, T_p is the temperature of the particles, u is the fluid velocity, u_p is the velocity of the particles, c_p is the specific heat capacity of the fluid at constant pressure, U is the fluid characteristic velocity, μ_0 and κ_0 are the fluid viscosity and thermal conductivity at initial temperature T_0, ρ is the density of clean fluid, γ_T is the temperature relaxation time, μ is the viscosity of clean fluid, σ is the electric conductivity of the fluid, P is the pressure acting on the fluid, N is the number of dust particles per unit volume, K is the Stokes constant, $K = 6\pi\mu D$, D is the average radius of dust
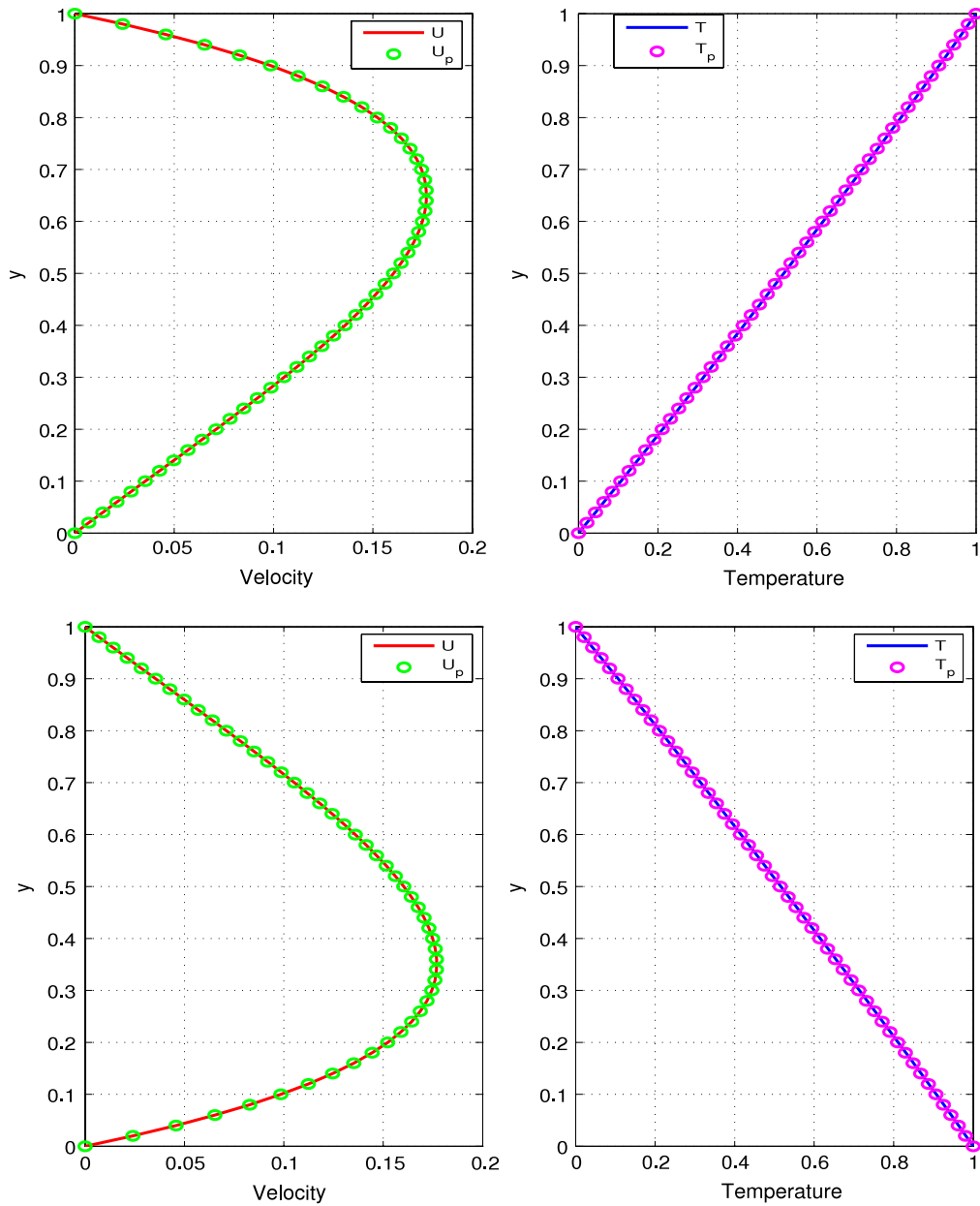
Fig. 3. Solutions with no-slip velocity and differential wall temperature.

particles. Ha is the Hartmann number, Re is the Reynolds number, R is the particle concentration parameter, G is the particle mass parameter, Ec is the Eckert number, Pr is the Prandtl number, a is the viscosity parameter, b is the thermal conductivity parameter, L is the temperature relaxation time parameter and β is the Navier slip parameter.

3. Numerical solution

Our numerical algorithm is based on the semi-implicit finite difference scheme given in [18] for the isothermal viscoelastic case. As in [19], we extend the algorithm to the temperature equation and take the implicit terms at the intermediate time level $(n + \xi)$ where $0 \leq \xi \leq 1$. The algorithm employed in [19] uses $\xi = 1/2$, we will however follow the formulation in [18] and thus take $\xi = 1$ in this article. For the case of constant viscosity and thermal conductivity, this formulation would correspond to a fully implicit scheme for the entire problem. The discretization of the governing equations is based on a linear Cartesian mesh and uniform grid on which finite differences are taken. We approximate both the second and first spatial derivatives with second order central differences. The equations corresponding to the first and
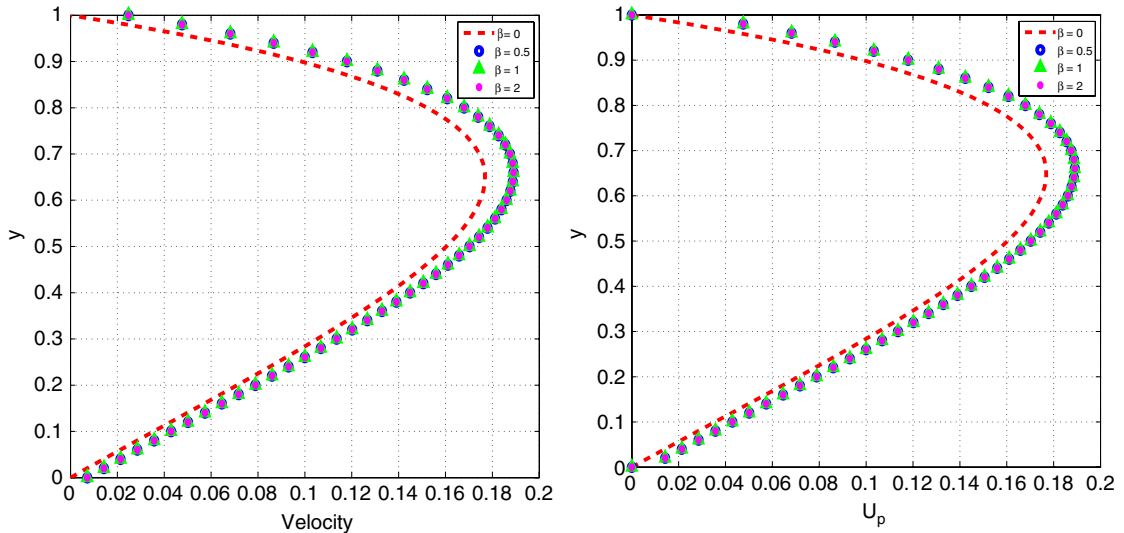
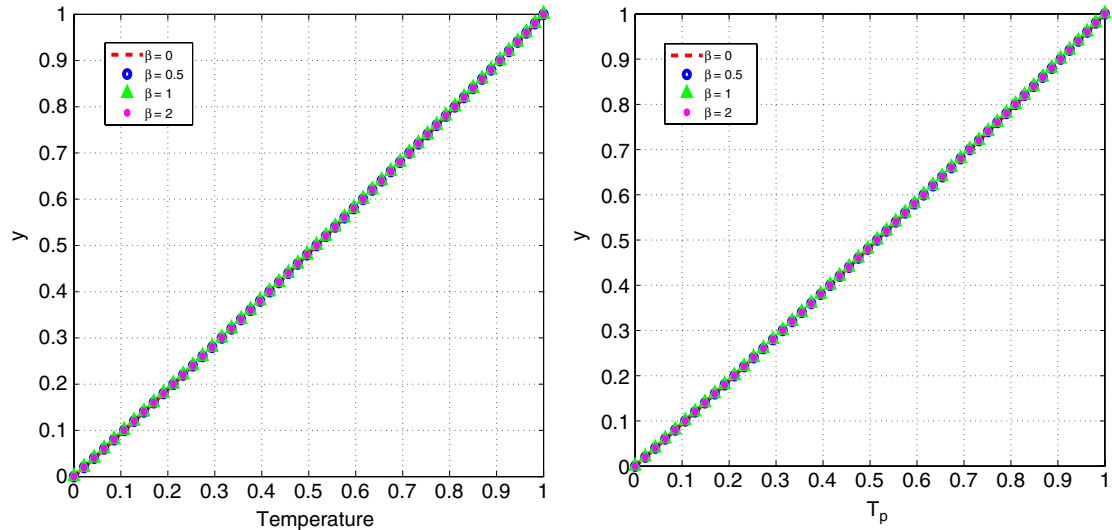**Fig. 4.** Evolution of longitudinal velocity.

Fig. 5. Evolution of temperature.

last grid point are modified to incorporate the boundary conditions. The semi-implicit scheme for the velocity component reads:

$$\text{Re}\frac{(u^{(n+1)} - u^{(n)})}{\Delta t} = \alpha\,\text{Re} + \mu_y^{(n)}\,u_y^{(n)} + \mu^{(n)}\,u_{yy}^{(n+\xi)} - (\text{Ha}^2 + R)u^{(n+\xi)} + Ru_p. \tag{11}$$

The equation for $u^{(n+1)}$ then becomes:

$$-r_1\,u_{j-1}^{(n+1)} + (1 + r_2 + 2r_1)\,u_j^{(n+1)} - r_1\,u_{j+1}^{(n+1)} = \text{explicit terms}, \tag{12}$$

where $r_1 = \mu^{(n)}\Delta t/(\text{Re}\,\Delta y^2)$ and $r_2 = \Delta t(\text{Ha}^2 + R)/\text{Re}$. The solution procedure for $u^{(n+1)}$ thus reduces to inversion of tri-diagonal matrices, which is an advantage over a full implicit scheme for the variable viscosity case. However, for the constant viscosity case our formulation is the same as a fully implicit scheme and the inversion of tri-diagonal matrices is retained. The semi-implicit integration scheme for the temperature equation is similar to that for the velocity component. Unmixed second partial derivatives of the temperature are treated implicitly:

$$\frac{T^{(n+1)} - T^{(n)}}{\Delta t} = \frac{1}{\text{Re}\,\text{Pr}}\left[\kappa_y^{(n)}\,T_y^{(n)} + \kappa^{(n)}\,T_{yy}^{(n+\xi)} - \frac{2R}{3}T^{(n+\xi)}\right] + \frac{\text{Ec}}{\text{Re}}[\mu\,u_y^2 + \text{Ha}^2\,u^2]^{(n)} + \frac{2R}{3\,\text{Re}\,\text{Pr}}T_p^{(n)}. \tag{13}$$
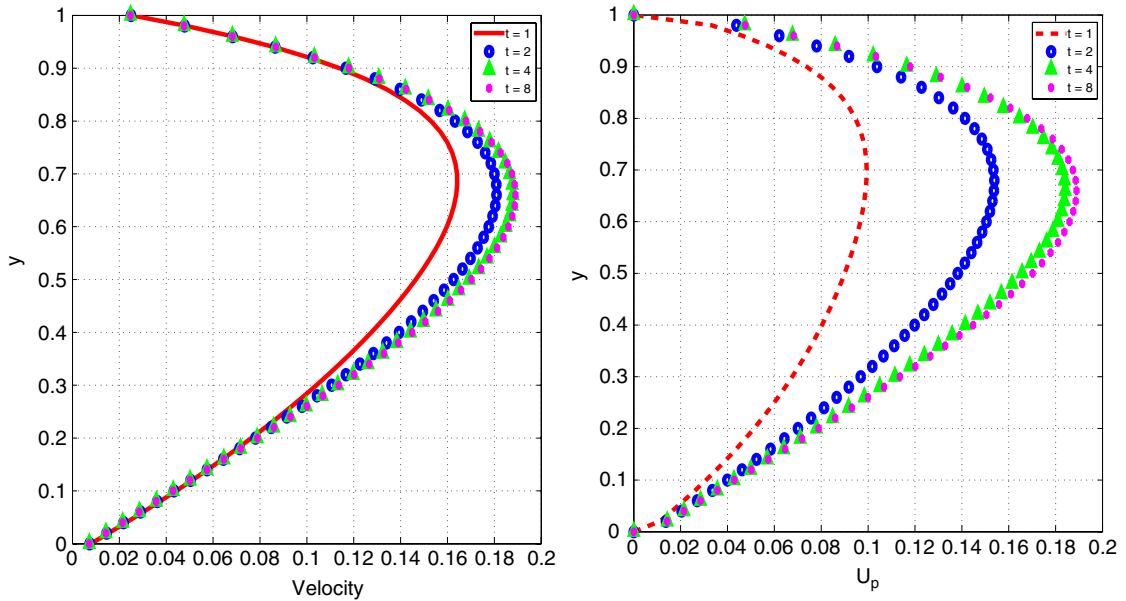
Fig. 6. Evolution of longitudinal velocity.

The equation for $T^{(n+1)}$ thus becomes:

$$- r_3 T_{j-1}^{(n+1)} + (1 + r_4 + 2r_3) T_j^{(n+1)} - r_3 T_{j+1}^{(n+1)} = \text{explicit terms,} \tag{14}$$

where $r_3 = \kappa^{(n)} \Delta t / (\text{Re Pr} \, \Delta y^2)$ and $r_4 = 2R \Delta t / (3 \, \text{Re Pr})$. The solution procedure again reduces to inversion of tri-diagonal matrices. The equations for u_p and T_p are linear and are thus solved implicitly.

$$\text{Re } G \frac{(u_p^{(n+1)} - u_p^{(n)})}{\Delta t} + u_p^{(n+\xi)} = u^{(n)}, \tag{15}$$

and

$$\frac{T_p^{(n+1)} - T_p^{(n)}}{\Delta t} + L T_p^{(n+\xi)} = L T^{(n)}. \tag{16}$$

The schemes (12) and (14) were checked for consistency. For $\xi = 1$, the (12)–(16) are first order accurate in time but second order in space. The schemes in [19] have $\xi = 1/2$ which improves the accuracy in time to second order. We use $\xi = 1$ here so that we are free to choose larger time steps and still converge to the steady solutions.

The algorithm was also tested for both spatial and temporal convergence and shown to be independent of both mesh size and time step size. In particular, if say the values $\Delta y = 0.05, 0.025, 0.02, 0.01$ are employed, our algorithm converges to the same solutions both qualitatively and quantitatively. Similarly using say 200,000 time steps and $\Delta t = 0.0001$ leads to the same quantitative/qualitative results as when using 80,000 time steps and $\Delta t = 0.00025$.

4. Results and discussion

Unless otherwise stated, we employ the parameter values: $R = 0.5$, $G = 0.8$, $\alpha = 1$, $a = 1$, $b = 0.01$, $\text{Pr} = 7.1$, $\text{Ec} = 0.2$, $\text{Re} = 1$, $L = 0.7$, $\beta = 1$, $\text{Ha} = 1$, $\Delta t = 0.0001$ and $t = 10$. It is important to note that the parameter a may take positive values for liquids such as water, benzene or crude oil. In some gases such as air, helium or methane, parameter a may be negative, i.e. the coefficient of viscosity increases with temperature. However, the most physically common case is $a > 0$, in which the fluid viscosity decreases with increasing temperature. Also, the parameter b may be positive for some fluids such as air or water vapor or negative for others such as liquid water or benzene. In the case $b < 0$, the fluid thermal conductivity would decrease with increasing temperature.

4.1. Code validation

If we run the code with zero boundary conditions for both the velocity ($\beta = 0$) and temperature ($T(1) = T(0) = 0$) then we would expect to recover symmetric parabolic profiles with maxima along the channel centerline. Fig. 2 displays these expected solutions.

The non-zero boundary condition at one of the walls clearly reduces the viscosity of the fluid close to that wall and thus we would expect the fluid adjacent to the hotter wall to flow much faster than that at the cooler wall, this is illustrated in Fig. 3; the top graph has a hotter upper wall and the bottom graph shows results for the reverse situation, a hotter lower wall.
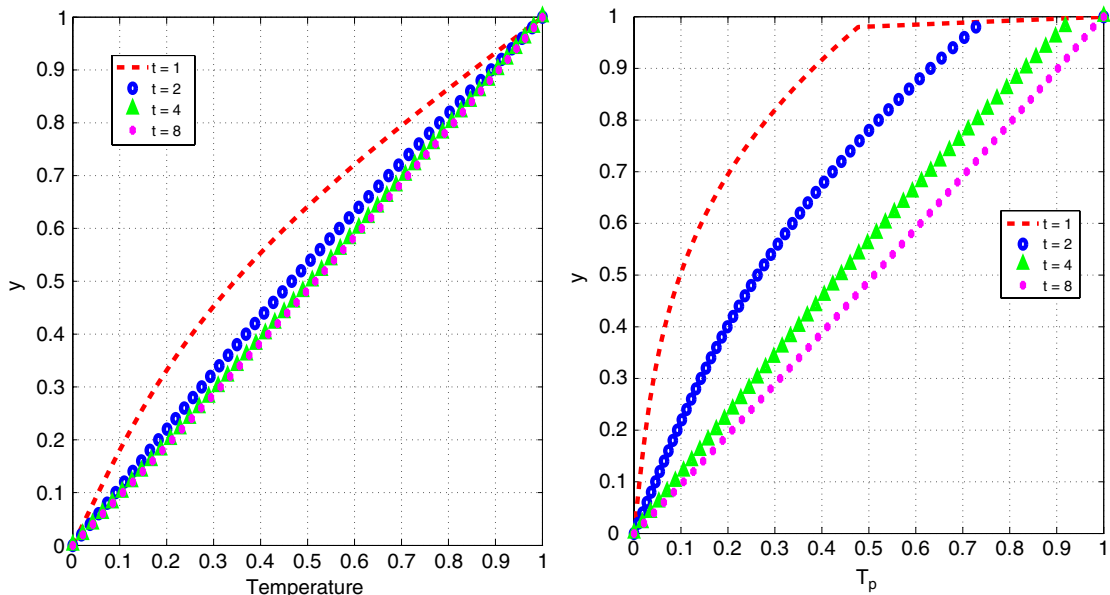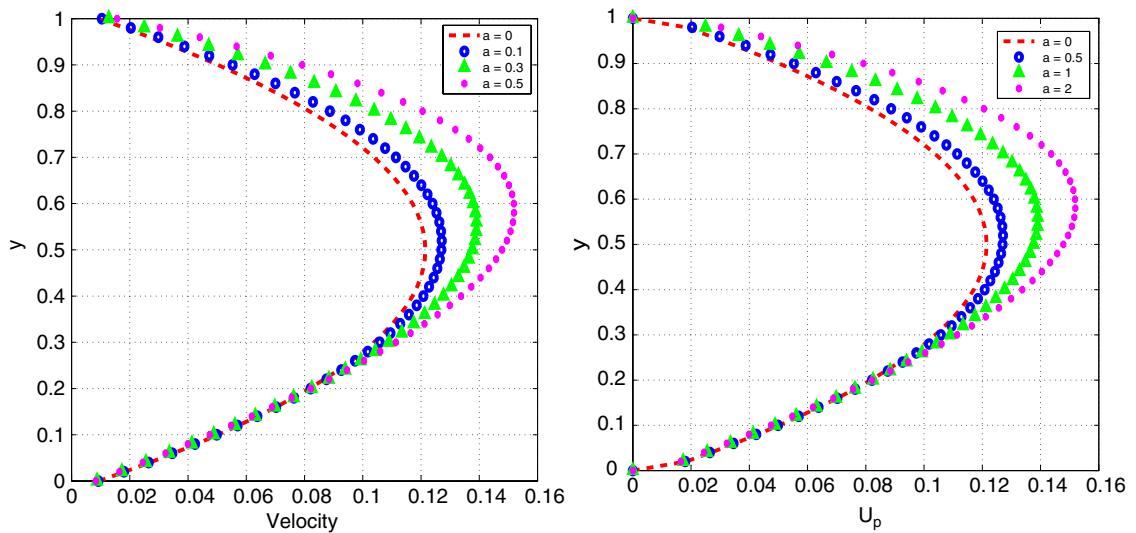
Fig. 7. Evolution of temperature.

Fig. 8. Evolution of longitudinal velocity.

The results for the remainder of the articles will correspond to the case of a hotter upper wall as given by the boundary conditions (8).

4.2. Effect of slip parameter

For non-zero values of β, the no-slip velocity condition no longer applies at either wall. Fig. 4 illustrates the slip condition at the wall for the longitudinal velocity. Due to the wall slip, the velocity is now predictably higher than that obtained under no-slip conditions. Under slip conditions, variation of the slip parameter seems to have minimal effects on the velocity field. The effects on the slip parameter of the temperature are quite minimal and barely noticeable for the chosen values, this should be expected since the temperature profiles are linear in convergence and there cannot be more than one linear field between any two given points (Fig. 5).

4.3. Transient solutions

The time dependent solutions show a progressive increase in both the velocity and temperature fields with time. This can be easily explained in terms of the rising temperature due to viscous heating among other heat sources included in
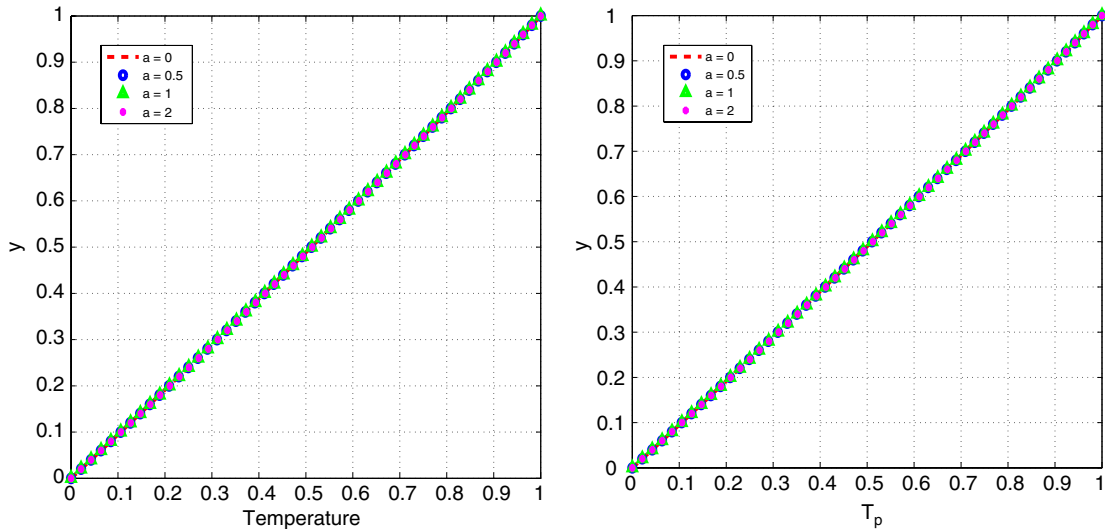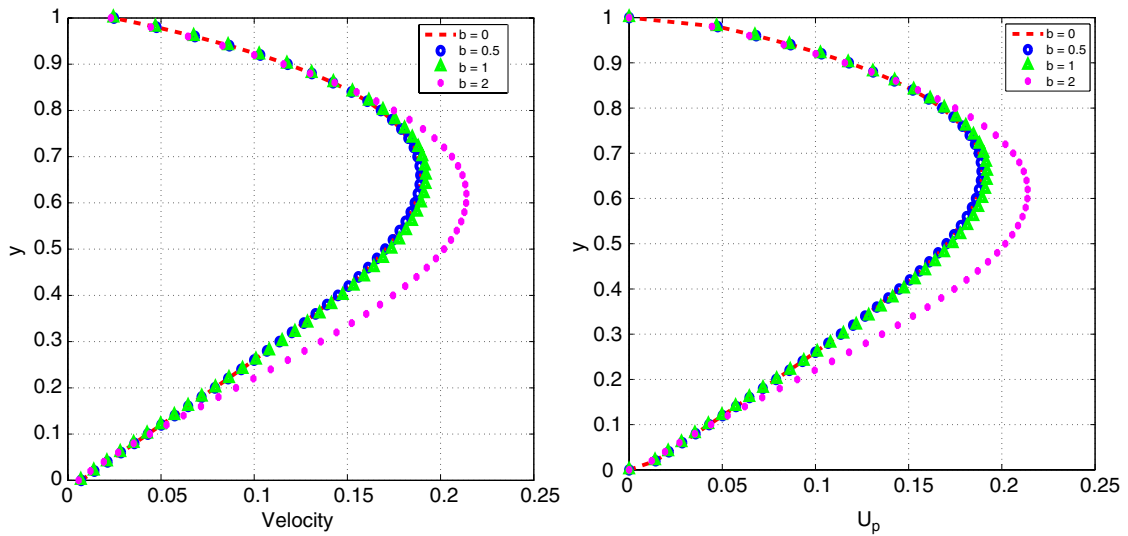
Fig. 9. Evolution of temperature.

Fig. 10. Evolution of longitudinal velocity.

our model. The rising temperature decreases the viscosity and hence leads to the noted velocity increase within the channel, as shown in Fig. 6. Once the temperature field has converged, no further reduction in the viscosity is expected and hence the velocity field will converge as well (Fig. 7).

4.4. Effect of viscosity variation

Lower viscosity fluid tends to move faster than that at higher viscosity and this is well illustrated in Fig. 8 (Fig. 9).

4.5. Effect of thermal conductivity variation

The linear temperature profiles that have been observed so far are only obtainable at relatively low conductivity parameters. Larger thermal conductivity parameter values lead to significant non-linearities in the physical model and these manifest in non-linear solutions which record higher temperatures within the channel, as shown in Fig. 11. The higher temperatures within the channel lead to lower viscosities and hence higher velocities, as illustrated in Fig. 10.

4.6. Effect of magnetic field

Fig. 12 shows that the velocity is reduced as the magnetic field strength is increased. Application of a transverse magnetic field to an electrically conducting dusty fluid gives rise to a resistive-type force called the Lorentz force. This force has the
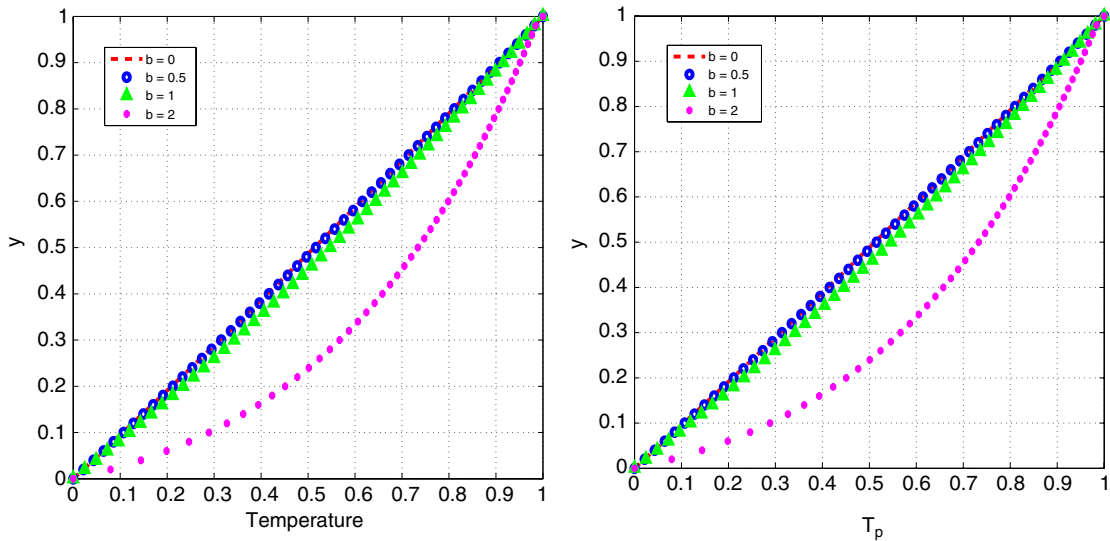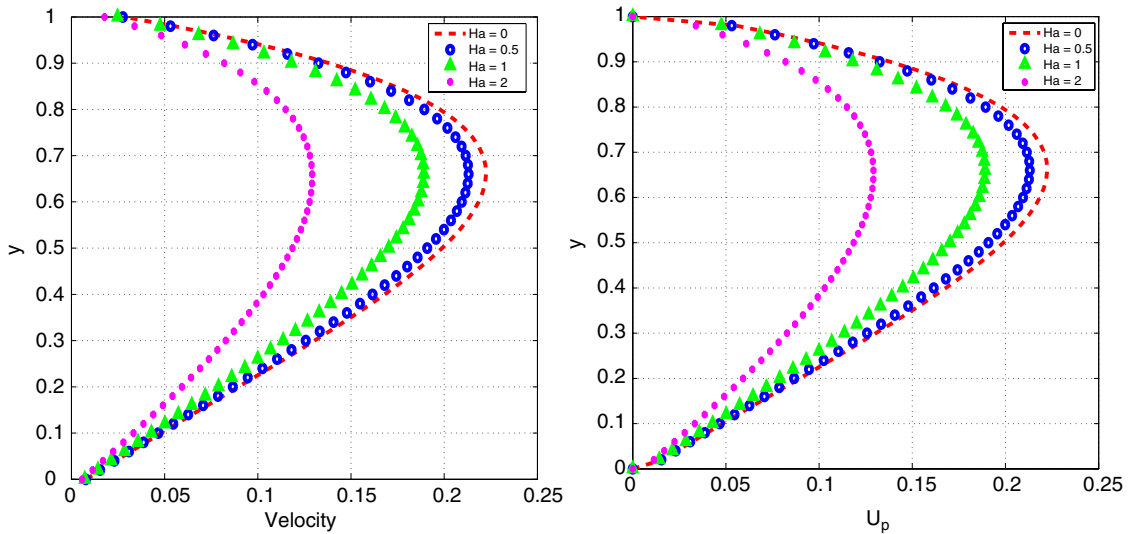
Fig. 11. Evolution of temperature.

Fig. 12. Evolution of longitudinal velocity.

tendency to slow down the motion of both the fluid and dust particles. Hence, an increase in Hartmann number presents a damping effect on the dusty fluid velocity profiles, as illustrated in Fig. 12. On the other hand, an increase in the Hartmann number due to magnetic field has no noticeable effect on the temperature distributions for the fluid and dust particles, as shown in Fig. 13.

5. Conclusion

We investigate the transient magneto-hydrodynamic flow of a fluid with temperature dependent viscosity and thermal conductivity. The fluid is subjected to one dimensional pressure driven flow under slip conditions at the walls. Starting from zero velocity and temperature conditions; we demonstrate, as expected, that the velocity and temperature fields progressively increase until a steady state is reached. Such steady solutions actually come much earlier than the time ($t = 10$) that is mostly used in this work. At higher thermal conductivity parameters, the temperature dependence of the thermal conductivity introduces strong non-linearities in the model and hence leads to nonlinear temperature profiles with higher recorded values. Decreases in the viscosity values either directly or indirectly (through increases in the temperature field) predictably lead to increased fluid velocities. The velocity fields of both the fluid and dusty particles tend to increase under Navier slip conditions while the temperature distributions are not affected. An increase in the Hartmann number results in an increasing damping magnetic force which decreases the velocities (u, u_p) and consequently the dissipations.
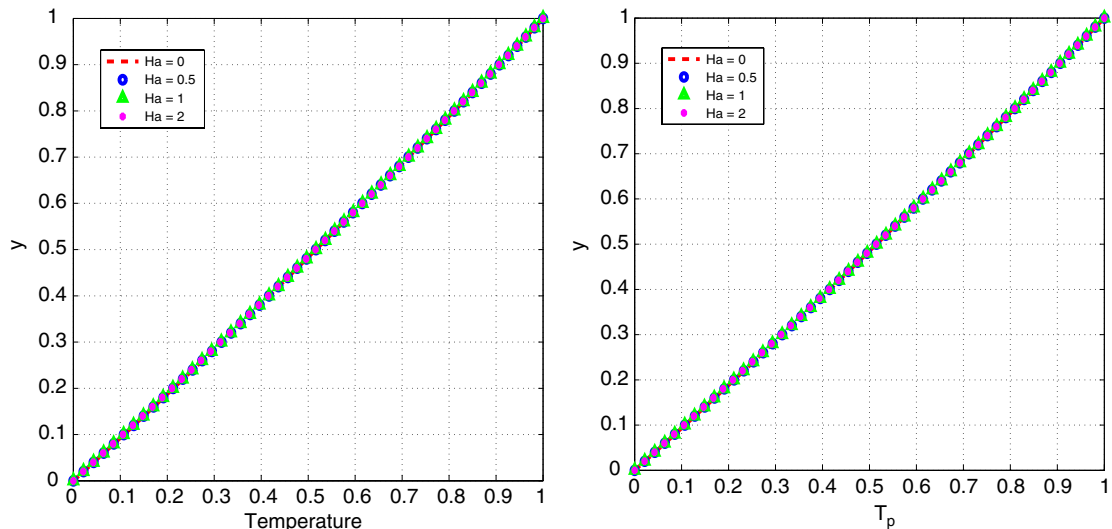
Fig. 13. Evolution of temperature.

As mentioned in the introduction, a number of significant applications of this work are found in the polymer industry and hence in the future we intend to extend the analysis presented herein to non-Newtonian fluids.

References

[1] P.G. Saffman, On the stability of a laminar flow of a dusty gas, J. Fluid Mech. 13 (1962) 120.
[2] R.K. Gupta, S.C. Gupta, Flow of a dusty gas through a channel with arbitrary time varying pressure gradient, J. Appl. Math. Phys. 27 (1976) 119.
[3] V.R. Prasad, N.C.P. Ramacharyulu, Unsteady flow of a dusty incompressible fluid between two parallel plates under an impulsive pressure gradient, Def. Sci. J. 30 (1979) 125.
[4] L.A. Dixit, Unsteady flow of a dusty viscous fluid through rectangular ducts, Indian J. Theor. Phys. 28 (2) (1980) 129.
[5] A.K. Ghosh, D.K. Mitra, Flow of a dusty fluid through horizontal pipes, Rev. Roumaine Phys. 29 (1984) 631.
[6] K.K. Singh, Unsteady flow of a conducting dusty fluid through a rectangular channel with time dependent pressure gradient, Indian J. Pure Appl. Math. 8 (9) (1976) 1124.
[7] P. Mitra, P. Bhattacharyya, Unsteady hydromagnetic laminar flow of a conducting dusty fluid between two parallel plates started impulsively from rest, Acta Mech. 39 (1981) 171.
[8] H.A. Attia, Unsteady MHD couette flow and heat transfer of dusty fluid with variable physical properties, Appl. Math. Comput. 177 (2006) 308–318.
[9] G.W. Sutton, A. Sherman, Engineering Magnetohydrodynamics, McGraw-Hill, 1965.
[10] H. Schlichting, Boundary Layer Theory, McGraw-Hill, 1968.
[11] M.T. Matthews, J.M. Hill, Newtonian flow with nonlinear Navier boundary condition, Acta Mech. 191 (3-4) (2007) 195.
[12] P.A. Thompson, S.M. Troian, A general boundary condition for liquid flow at solid surfaces, Nature 389 (1997) 360.
[13] Y.X. Zhu, S. Granick, Rate-dependent slip of Newtonian liquid at smooth surfaces-art. no. 096105, Phys. Rev. Lett. 8709 (9) (2001) 6105.
[14] W.F. Ames, Numerical Solutions of Partial Differential Equations, second ed., Academic Press, New York, 1977.
[15] O.D. Makinde, Effect of arbitrary magnetic Reynolds number on MHD flows in convergent-divergent channels, Internat. J. Numer. Methods Heat Fluid Flow 18 (6) (2008) 697–707.
[16] O.D. Makinde, P.Y. Mhone, On temporal stability analysis for hydromagnetic flow in a channel filled with a saturated porous medium, Flow Turbulence Combust. 83 (2009) 21–32.
[17] H. Herwig, G. Wicken, The effect of variable properties on laminar boundary layer flow, Warme- Stoffubertrag. 20 (1986) 47–57.
[18] T. Chinyoka, Y.Y. Renardy, M. Renardy, D.B. Khismatullin, Two-dimensional study of drop deformation under simple shear for Oldroyd-B liquids, J. Non-Newton. Fluid Mech. 31 (2005) 45–56.
[19] T. Chinyoka, Computational dynamics of a thermally decomposable viscoelastic lubricant under shear, Transactions of ASME, J. Fluids Engineering 130 (12) (2008) 121201 (7 pages).